Electronic Supplementary Material (ESI) for Chemical Communications

Supporting information

Synergetic promotion of photocatalytic activity of TiO_2 by gold deposition under UV-visible light irradiation

Junqing Yan, Guangjun Wu, Naijia Guan and Landong Li*

Key Laboratory of Advanced Energy Materials Chemistry (Ministry of Education), College of Chemistry, Nankai University, Tianjin 300071, P.R. China

* Corresponding E-mail: lild@nankai.edu.cn

Experiments and Methods

Preparation of TiO_2 and Au/TiO_2

All of the chemical reagents of analytical grade were purchased from Alfa Aesar Chemical Co. and used as received without further purification.

In a typical synthesis of anatase TiO_2, titanium tetrachloride ($TiCl_4$) was dropwise added into ice water under stirring to prepare a $TiCl_4$ aqueous solution with concentration of 1 mol/L. Then, 30 mL of $TiCl_4$ aqueous solution was mixed with 30 mL 1 mol/L KOH, and the resulting solution was transferred into a 75 mL Teflon-lined autoclave for static crystallization at 100 ^{o}C for 24 h. The obtained white

solid was centrifuged and thoroughly washed with deionized water, followed by drying in air at 80 ^{o}C for 24 h and calcination in a muffle furnace at temperatures of 400-700 ^{o}C for 12 h. The final products are denoted as TiO_2-n, where n represents the calcination temperature in centigrade.

Au clusters were loaded on the surface of TiO_2 through so called photo-deposition method. In a typical process, a certain amount of $HAuCl_4$ solution, 500 mg of TiO_2 and 10 mL of methanol were added into a round-bottom quartz flask under vigorous stirring to form slurry. The pH value of the slurry was adjusted to 10.5±0.2 using either 1M HCl or 1M NaOH aqueous solution and the slurry was irradiated by 250 W high-pressure mercury light with the main wavelength of 365 nm for 6 h under the protection of Ar. After irradiation, the solid particles were filtered, thoroughly washed and dried at ambient conditions.

Characterization of Au/TiO_2 samples

The specific surface areas of samples were determined through N_2 adsorption/desorption isotherms at 77 K collected on a Quantachrome iQ-MP gas adsorption analyzer.

The X-ray diffraction (XRD) patterns of samples were recorded on a Bruker D8 ADVANCE powder diffractometer using Cu-Kα radiation (λ= 0.1542 nm) at a scanning rate of 4 ^{o}/min in the region of 2θ = 20-80°.

Transmission electron microscopy (TEM) images were taken on a Philips Tecnai G^2 20 S-TWIN electron microscope at an acceleration voltage of 200 kV. A few drops of alcohol suspension containing the sample were placed on a carbon-coated copper

grid, followed by evaporation at ambient temperature.

Light absorption spectra of samples (*ca.* 100 mg) were recorded in the air against $BaSO_4$ in the region of 200-700 nm on a Varian Cary 300 UV-Vis spectrophotometer.

X-ray photoelectron spectra (XPS) were recorded on a Kratos Axis Ultra DLD spectrometer with a monochromated Al-Ka X-ray source (*hv* = 1486.6 eV), hybrid (magnetic/electrostatic) optics and a multi-channel plate and delay line detector (DLD). All spectra were recorded using an aperture slot of 300*700 microns, survey spectra were recorded with a pass energy of 160 eV and high-resolution spectra with a pass energy of 40 eV. Accurate binding energies (±0.1 eV) were determined with respect to the position of the adventitious C 1s peak at 284.8 eV.

Electron spin resonance (ESR) was carried out on a Bruker A300 instrument with a microwave power of 5.0 mW and a modulation frequency of 100 kHz. 2,2-diphenyl-1-picrylhydrazyl hydrate (DPPH) was used as an internal standard for the measurement of the magnetic field. In a typical experiment, sample of 0.15g was placed in a quartz ESR tube and evacuated at 473 K for 2 h. After cooled down to 298 K, 50 Torr O_2 was introduced to the cube and kept for 15 min. The excess amount of O_2 was removed from the tube by evacuation for 10 min and then the tube was analyzed at 100 K. The control experiments were carried out without O_2 treatment. All treatments were done in dark.

The photocatalytic generation of OH radicals under irradiation was measured by the fluorescence method using the terephthalic acid (TA) as a chemical trap ($\cdot OH + \text{terephthalic acid} \rightarrow \text{2-hydroxyterephthalic acid}$). Typically, 0.01g

photocatalysts was dispersed in 50 mL aqueous solution containing $5x10^{-4}$ M terephthalic acid, $2x10^{-3}$ M NaOH at 298 K and irradiated under UV, visible and UV-visible light. Fluorescence emission intensity of generated 2-hydroxyterephthalic acid at about 425 nm was measured on a Hitachi F-4500 fluorescence spectrophotometer every 15 min under the excitation at 320 nm.

Photocatalytic evaluation

Photocatalytic reforming of methanol (also-known as photocatalytic water splitting with methanol as sacrificial agent) was performed in a top-irradiation-type Pyrex reaction cell connected to a closed gas circulation and evacuation system under the irradiation of Xe lamp (wavelength: 320-780 nm) with different optical filters. In a typical experiment, catalyst sample of 100 mg was suspended in 100 mL 10 % methanol aqueous solution in the reaction cell. After evacuated for 30 min, the reactor cell was irradiated by the Xe lamp at 200 W under stirring. The gaseous products were analyzed by an on-line gas chromatograph (Varian CP-3800) with thermal conductivity detector.

Figures and Tables

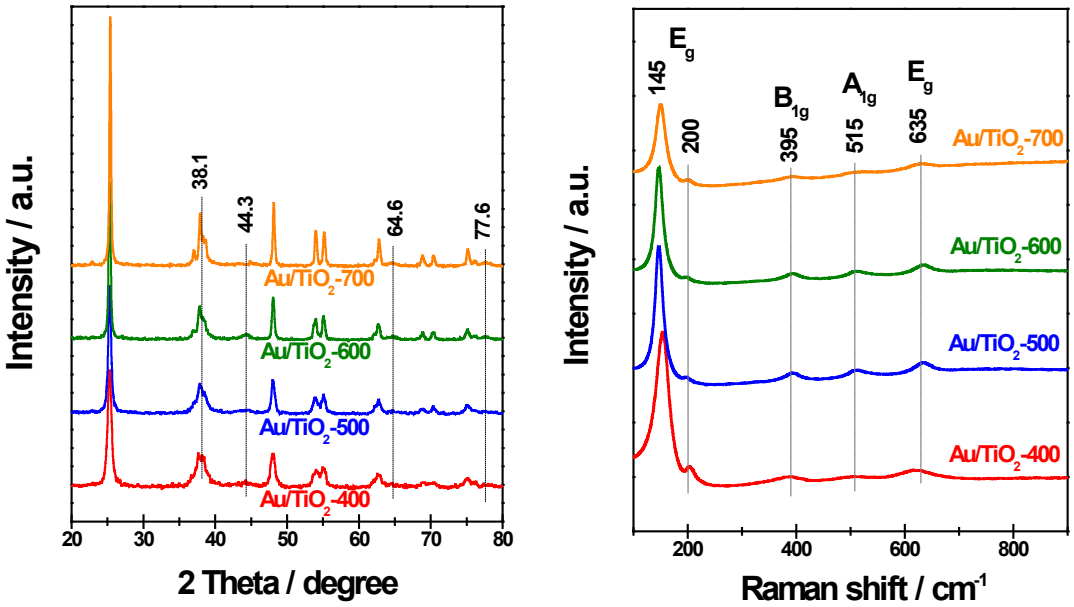

Figure S1 XRD patterns and Raman spectra of Au/TiO_2 samples

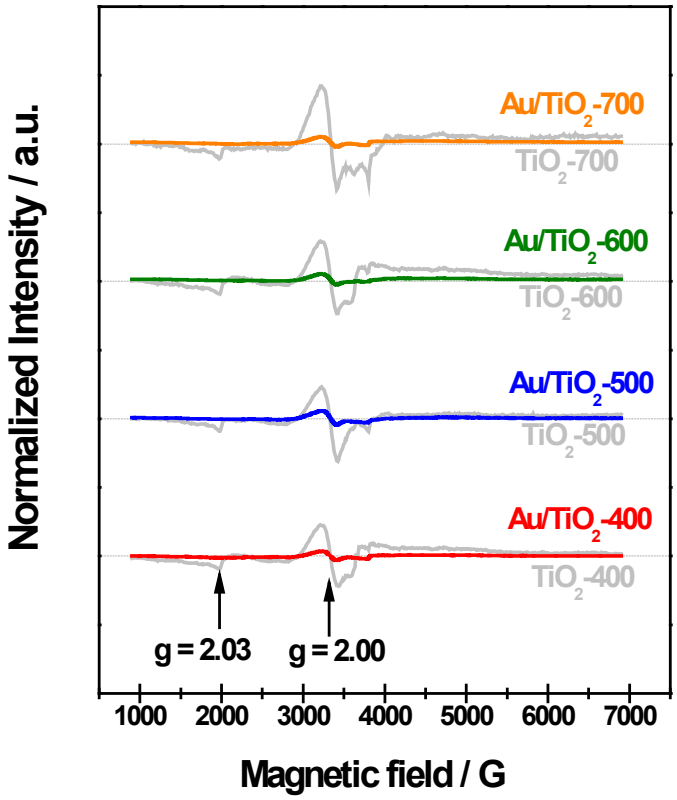

Figure S2 ESR results of the Au/TiO_2 and TiO_2 samples

The samples were evacuated at 473 K and then treated with 50 Torr O_2 at 298 K. The samples were measured at 100 K in dark.

As shown in Figure S2, all anatase TiO_2 samples show two signals, at g=2.00 and g=2.03, which could be assigned to O^- formed through O_2 dissociative adsorption onto the surface oxygen vacancy sites of TiO_2, i.e. so-called surface defects [S1-S4]. Without O_2 pretreatment, no ESR signals could be detected for all samples, confirming that the signals are from the O^-. After surface area normalization, the intensity of ESR signals can reflect amount of defects per surface area, i.e. the density of surface defects. The ESR signals decline dramatically with the loading of Au

nanoparticles on the surface of TiO_2 (in consistence with ref. [S3]), indicating that Au nanoparticles locate on surface defect sites. This is also in accordance with the fact that the surface defect sites are the trapping centers of photo-generated electrons, which could reduce Au cations during photo-deposition. In another word, the surface defects are the nucleation sites for Au during photo-deposition. Undoubtedly, higher density of nucleation sites will lead to smaller size of Au nanoparticle.

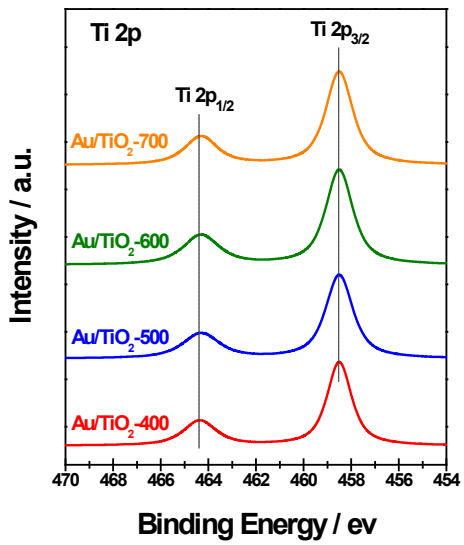

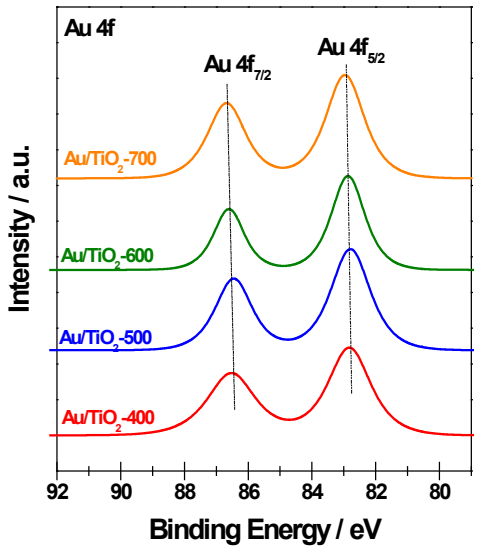

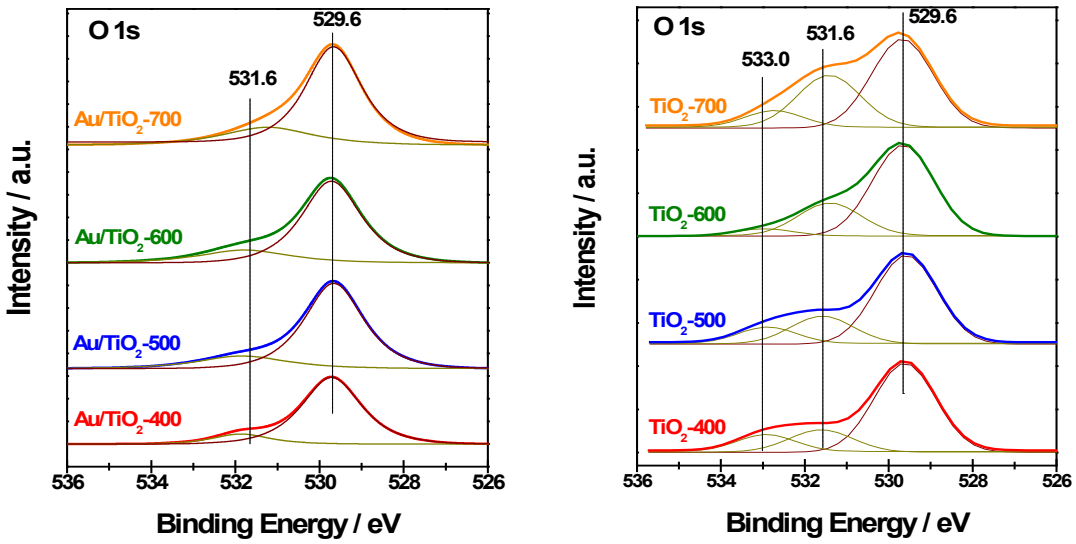

Figure S3 Au 4f, Ti 2p and O 1s XP spectra of Au/TiO_2 samples, and Ti 2p, O 1s XP spectra of TiO_2

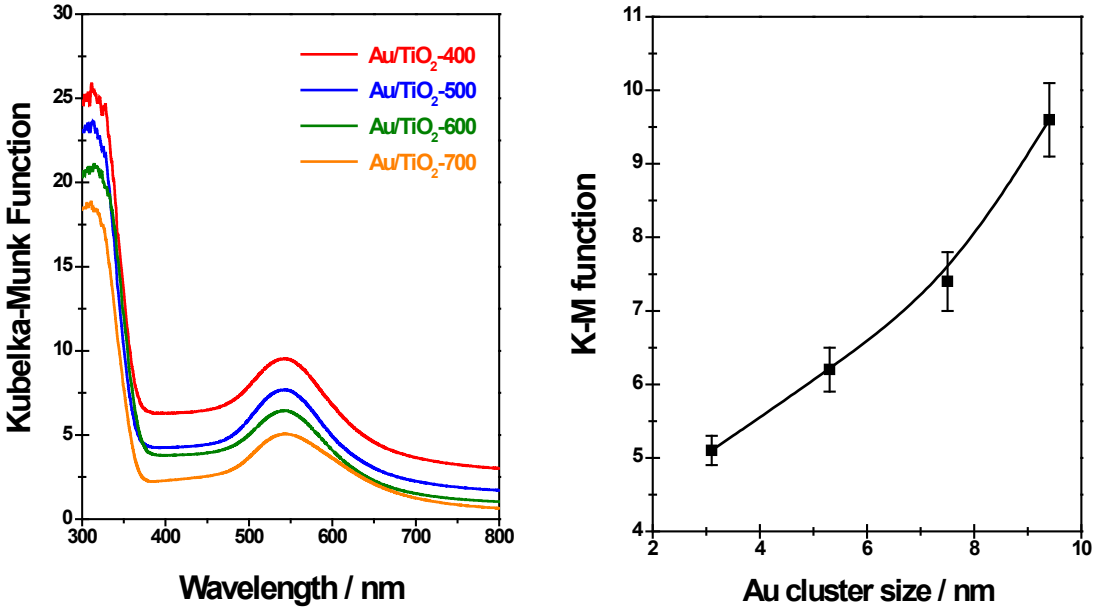

Figure S4 Light absorption spectra of Au/TiO_2 samples and the relationship between the absorption intensity of the SPR band at λ=550 nm and Au particle size

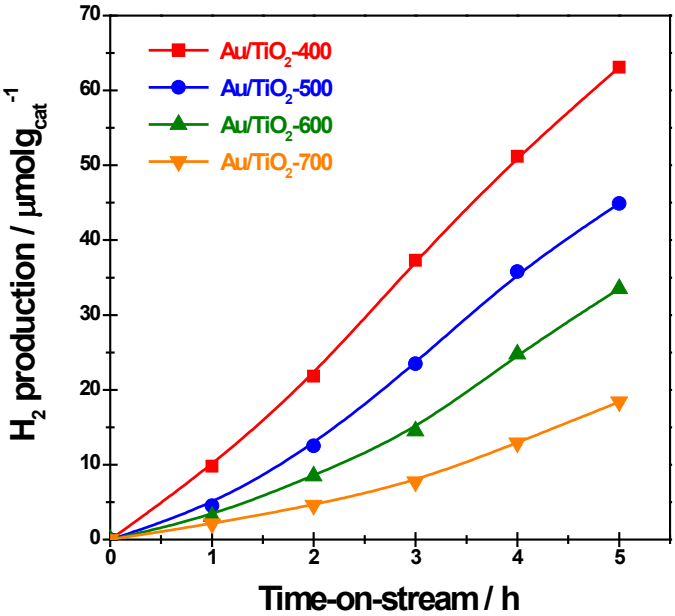

Figure S5 Hydrogen evolution during methanol photocatalytic reforming over Au/TiO_2 samples under visible light (400~780 nm) irradiation

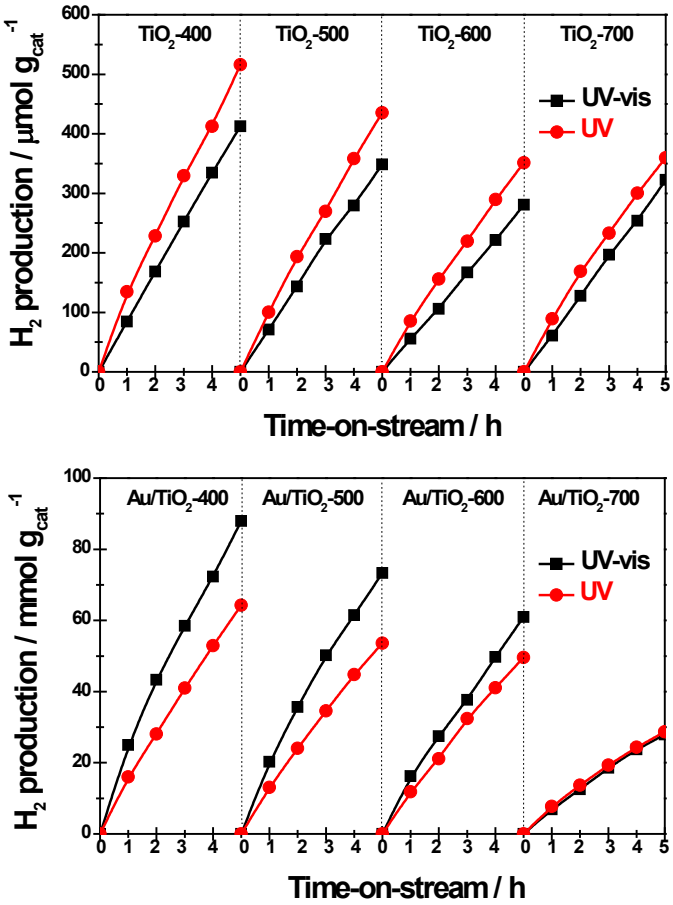

Figure S6 Hydrogen evolution during methanol photocatalytic reforming over TiO_2 and Au/TiO_2 samples under UV (320~400 nm) and UV-Vis (320~780 nm) light irradiation

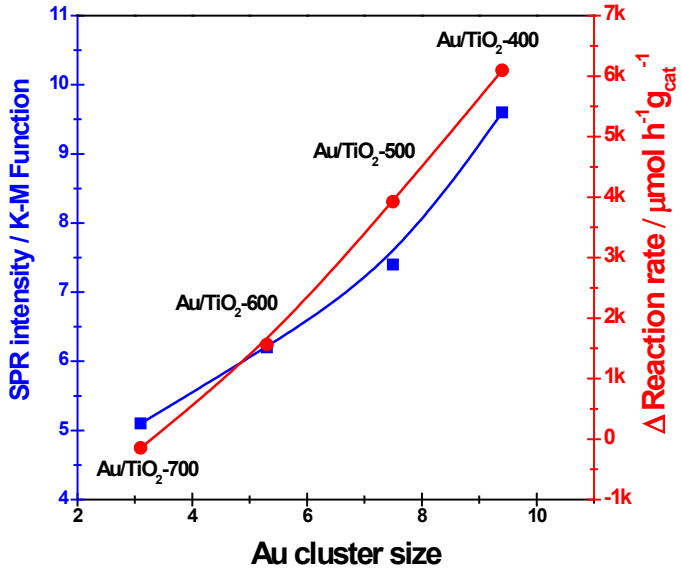

Figure S7 The relationship between the SPR intensity of Au nanoparticles and Δ reaction rate (Δ= $Rate_{UV\text{-}Vis}$ – $Rate_{UV}$ - $Rate_{Vis}$)

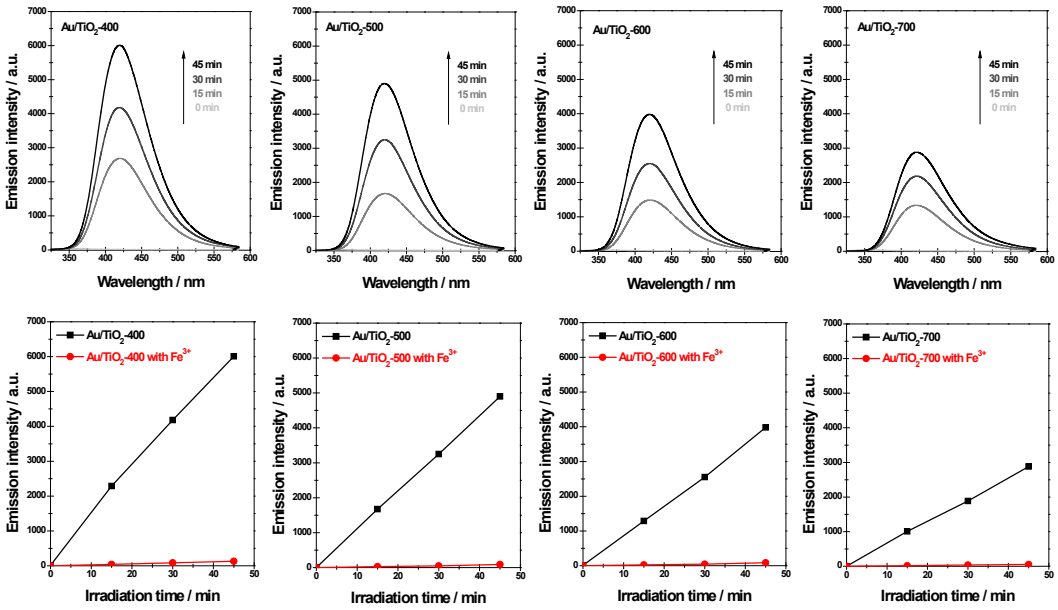

Figure S8 Fluorescence spectra of Au/TiO_2 under UV light irradiation and the time-dependent fluorescence intensity at 426 nm with/without the presence of Fe^{3+}

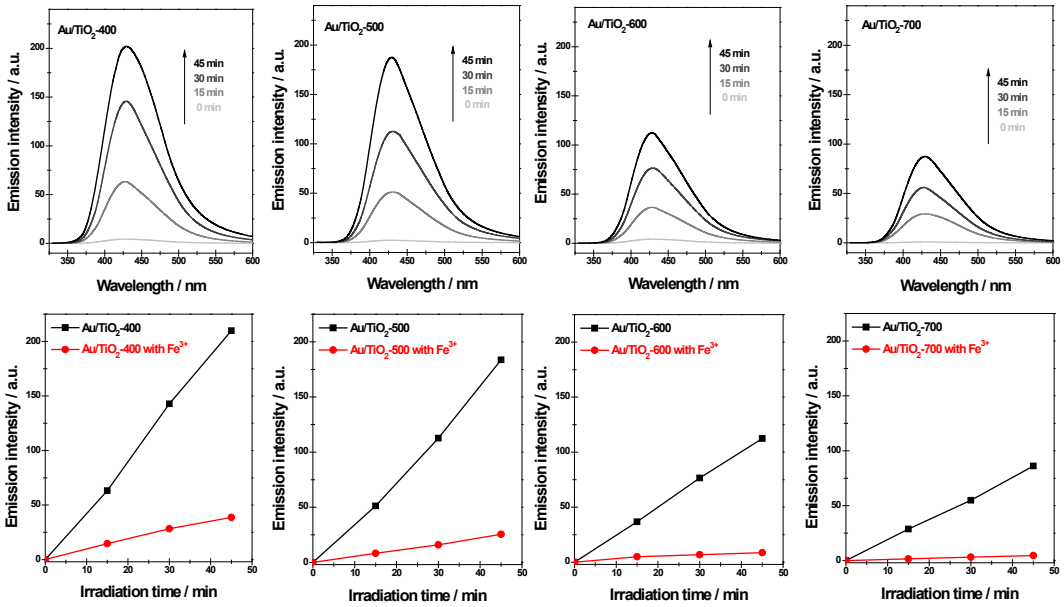

Figure S9 Fluorescence spectra of Au/TiO_2 under visible light irradiation and the time-dependent fluorescence intensity at 426 nm with/without the presence of Fe^{3+}

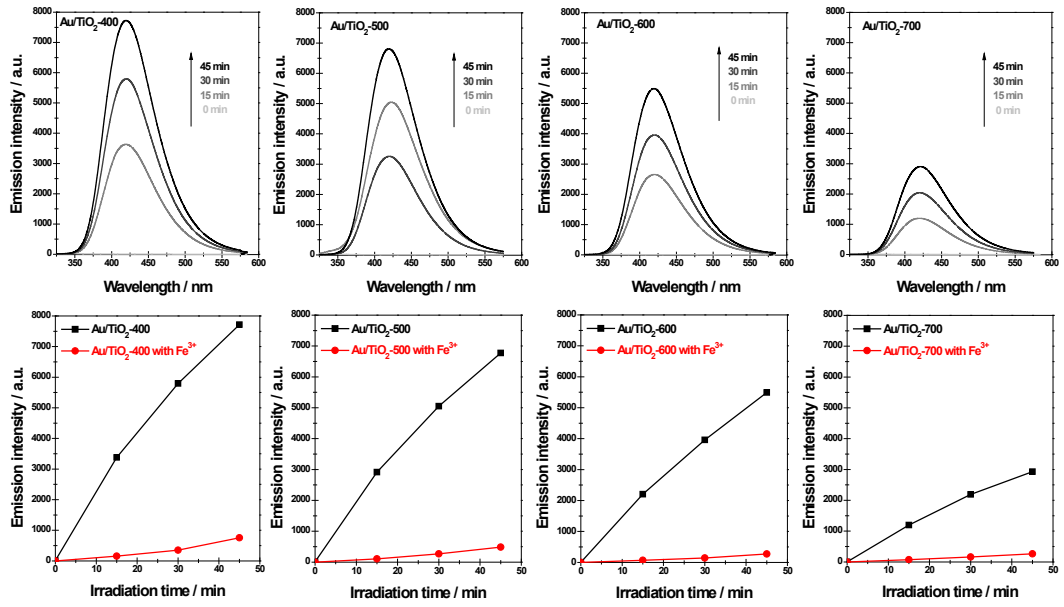

Figure S10 Fluorescence spectra of Au/TiO_2 under UV-visible light irradiation and the time-dependent fluorescence intensity at 426 nm with/without the presence of Fe^{3+}

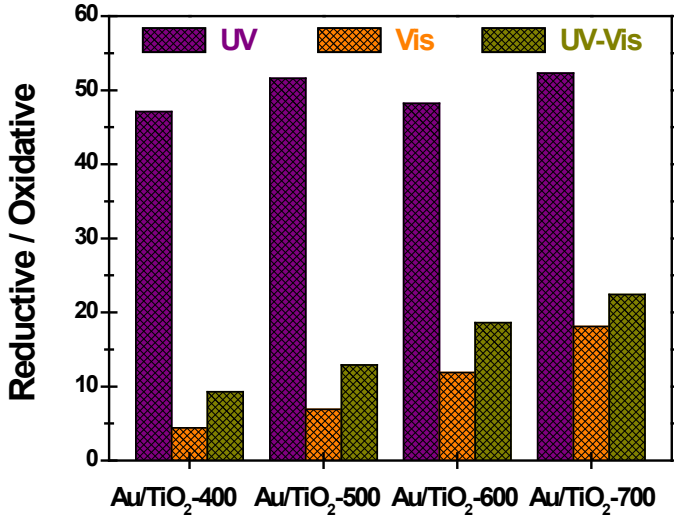

Figure S11 The formation of OH radicals from the reductive and oxidative pathway under different irradiations as determined by fluorescence spectra

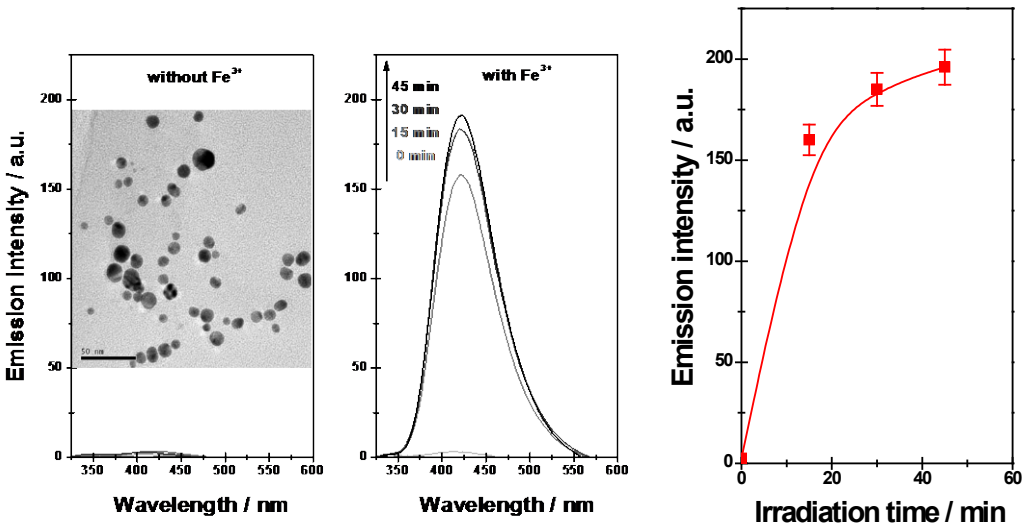

Figure S12 Fluorescence spectra of Au colloid under visible light irradiation and the time-dependent fluorescence intensity at 426 nm in the presence of Fe^{3+}

Inlet: TEM of Au colloid

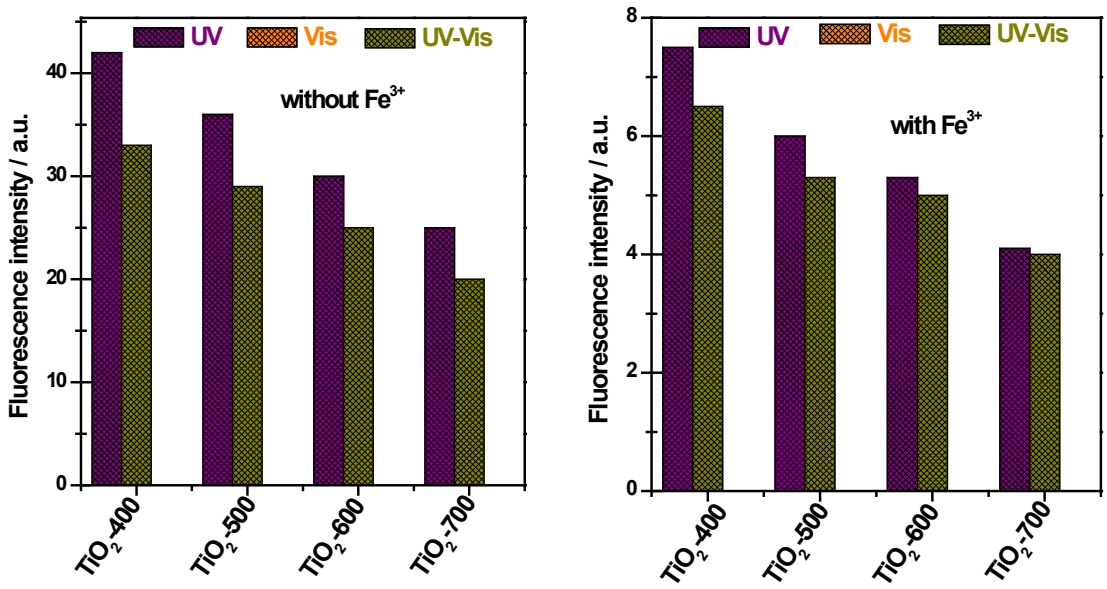

Figure S13 Fluorescence intensity caused by trapped OH radicals at time-on-stream of 30 min with/without the presence of Fe^{3+} under different irradiations

Table S1 Physicochemical properties of Au/TiO_2 samples under study

Samples	Size (nm) [a]		Au	S_{BET}	Hydroxyl groups % [c]		
	TiO_2	Au	wt.% [b]	(m^2/g)	Before PD	After PD	Δ [d]
Au/TiO_2-400	16.6	9.4	3.94	121.6	30.5	17.1	13.4
Au/TiO_2-500	19.4	7.5	3.97	69.4	36.6	18.8	17.8
Au/TiO_2-600	26.8	5.3	3.92	43.3	42.3	17.6	24.7
Au/TiO_2-700	36.5	3.1	3.95	20.9	49.3	16.2	33.1

[a] Average size estimated from TEM observation

[b] Measured by ICP

[c] Estimated from O 1s XP spectra

[d] Difference in the percentage of hydroxyl groups before and after photo-deposition

References

[S1] I. Fenoglio, G. Greco, S. Livraghi and B. Fubini, Chem. Eur. J. 2009 , 15 , 4614.

[S2] J. M. Coronado and J.Soria, Catal. Today, 2007, 123, 37.

[S3] Y. Shiraishi, D. Tsukamoto, Y. Sugano, A. Shiro, S. Ichikawa, S. Tanaka and T. Hirai, ACS Catal., 2012, 2, 1984.

[S4] D. Tsukamoto, Y. Shiraishi, Y. Sugano, S. Lchikawa, S. Tanaka and T. Hirai, J. Am. Chem. Soc., 2012, 134, 6309